

The Design and Fatigue Life Prediction for a Speed-Reduction Device

Yuo-Tern Tsai^{a*}, Kuan-Hong Lin^{**} and Kuo-Shong Wang^{***}

Key words: fatigue life, reliability, FEM, reducer.

ABSTRACT

This paper presents the methods of structural stress analysis and fatigue-life prediction for a reducer possessing high reduction ratios. It contains (1) the design and kinematic simulation of an eccentric cam reducer, (2) the analyses of root bending stress (**RBS**) and surface contact stress (**SCS**) of the reducer based on ISO standard 6336-3, (3) the predictions of bending and contact fatigue lives of the reducer based on ANSI/AGMA models and a linear model, and (4) the finite element stress analysis of the reducer combining with a fatigue-life and reliability analysis. The analyzed stresses in finite element methods (**FEM**) are compared with those in formula calculation to identify the accuracy of the geometric models. The fatigue lifetimes of the reducer predicted by the ANSI/AGMA and the proposed models are compared to identify the feasibility of the prediction model. Reliability degradation of the reducer at different loads is further studied for giving the risks within the preset used times. The analyzed results show that failures of the reducer are primarily incurred by the bending stress. The studied results are useful in designing, structural stress analysis and fatigue-life prediction for developing a high ratio speed-reduction device.

1. INTRODUCTION

Reducers are extensively applied for speed reduction in many types of machinery such as machine tools, transmission mechanisms and robots, etc. The functional properties, such as speed-reduction ratio, transmitted torque and efficiency frequently are requested to satisfy the applied needs, especially for robotic devices. The harmonic gear decelerator is often

used in robotic devices because it has the properties of small backlash, high transmission accuracy, and large reduction ratio (Taghirad et al., 2009). The problems of harmonic gear decelerators are their rigidity and limited transmitted torque due to the flexible design of the gear rings (Ghorbel et al., 2001). The other frequently applied type is the trochoidal gear reducer which has the advantages of high torsional rigidity, greater loading capacity and high shock-resistant ability. The design and strength analysis of a trochoidal gear reducer have been reported by (Shuting, 2014). Although many types of reducers have been designed and used in current, many structural problems such as motion, stress and fatigue-life, still need further to be solved for engineering applications

The reducer is designed with simple components so that a good cost-performance ratio can be obtained (Tsai et al., 2004). It is mainly consisted of four components including one off-center cam and several gear rings. The gear rings play a critical role in determining the speed-reduction ratios and the allowable loadings. The failure modes of the gear rings are either gear tooth breakage or pitting of the tooth surface incurred by the working stresses. Gear tooth breakage is caused by internal stress rupturing which is a direct result of the accumulated residual stress or root bending stress exceeding the strength of the material (Alban, 2008). Surface pitting, including detachment of fragments of material can occur due to repeated contact stress. It normally starts with surface distress which, in severe cases, may develop into spalling. A secondary crack may start from a spalling crater and propagate through the thickness of the tooth, finally resulting in a part of the tooth falling off. The general approach to reinforcing the gear strength as well as improving quality is by heat processing (Kader et al., 1998). The studies about gear design and analysis have been reported by some associations such as the Japanese Gear Manufacturers Association (JGMA, 1975) and American Gear Manufacturers Association (AGMA, 2004). Typically, Thompson et al. (2000) presented a trade-off in the analysis of minimum volume design for multi-stage spur gears.

The fatigue life usually varies depending upon

Paper Received April, 2017. Revised May, 2018. Accepted May, 2018. Author for Correspondence: Yuo-Tern Tsai. Email: ytttsai@mail.hdut.edu.tw

** Professor, Department of Mechanical Engineering, Hungkuo Delin University of Technology, 236, Taiwan, R.O.C.*

*** Professor, Department of Mechanical Engineering, Tunghan University, 222, Taiwan, R.O.C.*

**** Professor, Department of Mechanical Engineering, National Central University, Chungli, Taiwan, ROC.*

the material strength, tooth size, hardening process, and so on. To obtain the expected life, considering stress concentration and fatigue resistance in designing are necessary. The methods of numerical optimization for stress concentration and fatigue life of gears had been presented by Ciavarella and Demelio (1999). Normally, fatigue failures are a result of cumulative damage caused by repeated or fluctuating stresses. The most common method to estimate the fatigue life is by the S-N curves of materials (Lee et al., 2005). Fatigue stresses of gear teeth include both Root Bending Stress (**RBS**) and Surface Contact Stress (**SCS**). Evaluating the **RBS** and the **SCS** of the gear rings are critical in predicting fatigue failures of the reducer. The evaluations of the two stresses always involve many unknown parameters which are associated with the operational environments (ISO 6336, 1996). For a design engineer, the often arisen problems in evaluation are how to give proper values to these unknown parameters.

The evaluated models of fatigue life of gears had been reported in AGMA. The models were formulated based on S-N curve graphs in terms of stress cycle factors. An often used approach in analyzing structural stresses is by finite element methods (**FEM**). The **ANSYS** is a tool of **FEM**, which has been extensively applied in many fields Robert (2001). The geometric models created by **CAD** can be imported into **ANSYS** for meshing and performing statistical and dynamic analyses (ANSYS, 2012). It is sometimes difficult to obtain an optimal solution with **FEM** due to the definitions slightly violating the constraints but the efficiency can be improved by replacing the search algorithms. Recently, the use of **FEM** to perform engineering stress analysis and support product design has been extensively studied. For example, Tsai et al.(2013) made use of the limited experimental data and simulated stress obtained by **FEM** to evaluate the fatigue life of dental implants. The integration of **CAD/CAE** with probabilistic theories to perform reliability optimization design for robotic arms is another example (Tsai et al., 2013).

This paper reports the design concepts of a new speed-reducer including motion simulation, stress analysis and fatigue life prediction. Geometric models of the reducer are designed using parametric methods so that the related components can be rapidly created while designing. The **RBS** and **SCS** of the gear rings are evaluated based on the ISO 6336 standards. The **FEM** is used to obtain the maximum **RBS** and **SCS** of the gear rings under various loadings. The analyzed results are used to decide the allowable loadings of the reducer. A linear model based on the S-N curve is proposed for predicting the fatigue lifetimes. The estimated lifetimes are compared with those obtained by the AGMA models. The studied results

showed that the bending fatigue failures will occur faster than the contact fatigue failures. The reliabilities of fatigue life are further investigated for giving the risks of the reducer in use under various loadings.

2. THE REDUCER

A new gear reducer is proposed for obtaining the properties of high rigidity, large reduction ratios and small volume. The motion is simulated to observe the kinematic properties of the reducer.

2.1 Design concepts

The working principles of the reducer are designed based on differential displacement of gear rings which is similar to the movement of the sliding meter to the fixed meter of the traditional calipers. There are four main components enclosed in the reducer, the fixed ring, sliding ring, intermediary ring and off-center cam. An isotropic view of the reducer is illustrated in **Figure 1**.

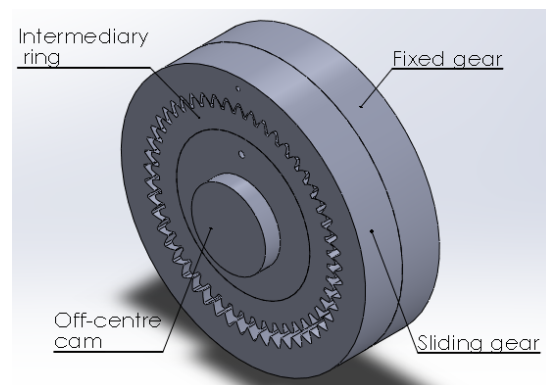


Figure 1. Geometric structure of the reducer

The fixed ring is fixed onto a support box for guiding the rotation of the intermediary ring as planetary motion. The intermediary ring is driven by the off-center cam for transmitting the power from the input shaft to the sliding ring. The fixed and sliding rings are designed with different teeth so that a slight difference of position of the two paired teeth is generated when the intermediary ring is rotating along the fixed ring. The paired teeth are forced to align with each other by the teeth of the intermediary ring. The differential displacement results in a large speed-reduction ratio of the sliding ring to the input shaft. The ratios of speed-reduction are dependent on the difference of the number of teeth on the fixed and sliding rings.

The off-center cam is driven by the power shaft which is installed inside the intermediary. It rotates to drive the intermediary ring for the generation of planetary motion along with the fixed ring. The off-center cam can be designed with a counterweight on the other side to alleviate any imbalance during

rotation. The teeth of the gear rings are designed with a profile-shifted involute to avoid the occurrence of interference. The bearings of the power shaft can be settled on either side of the support box for a more compact structure.

The teeth of the gear rings are created using a parametric approach which is programmed using the macros in the SolidWorks software. This parametric design approach ensures that the teeth can be created rapidly according to the attributes such as number of teeth, modules, compressive angle and the profile-shifted values, etc. The number of teeth is decided according to the speed-reduction ratio.

2.2 Kinematic properties

The motion simulation is carried out using the SolidWorks for interference check and velocity analysis. The teeth of the gear rings are designed with an involute profile where the module is $m=1$ and the pressure angle $\theta=20^\circ$. The fixed, sliding and intermediary gear rings in this example are designed with 50, 49, and 48 teeth, respectively. The ratio of speed-reduction for this design would be $s = -1/49$. The off-centre cam is designed according to the geometry of the paired transmission of the gear rings. The off-centre distance is defined as

$$e = \frac{D_c - D_s}{2}, \tag{1}$$

where D_s, D_c are the pitch diameters of the sliding and the fixed gears, respectively.

The ratio of speed reduction is decided depending upon the number of teeth of the gear rings. The ratio of speed reduction can be expressed as

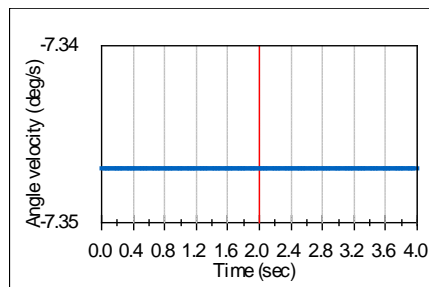
$$s = \frac{z_s - z_c}{z_s}, \tag{2}$$

where z_s, z_c stand for the number of teeth on the sliding and fixed rings, respectively.

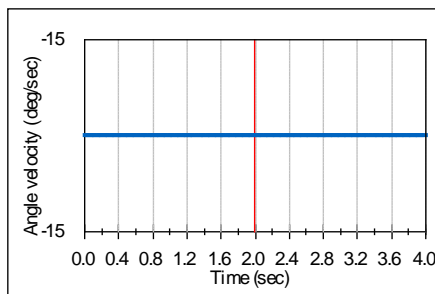
The simulated results show that the design in tooth number, tooth shape and assembly are practical. The simulated time is set to 4 sec and the rotational speed of the off-centre cam is set to $n_i=360^\circ/s$ (60 rpm). The simulation results for the angle velocity of the gear rings are shown in **Figure 2**. The ratio of the angle velocity of the sliding ring to the off-centre cam is equal to the speed-reduction ratio, $s=-1/49$. In contrast, the speed ratio will be $s=1/50$ if the reducer is designed with gear numbers of $z_s=50$ or $z_c=49$.

The loadings are added on the sliding ring as well as the driven torques on the off-center cam to simulate the mechanical benefits and the needed power torque. The simulation results for the power torque and power consumption at a loading of 100 Nm are shown in **Figure 3**. The power torque and power consumption needed given the loading conditions are 2.04 Nm and 1.28 watts, respectively. The scale of the power torque

to the loading torque is just equal to the speed-reduction ratio (1/49). Here, the simulated results are obtained based on the ideal conditions which neglect the effects of frictional forces. The motion simulation not only identifies the feasibility of the design but also provide rough information about the needed power for the drive motors.

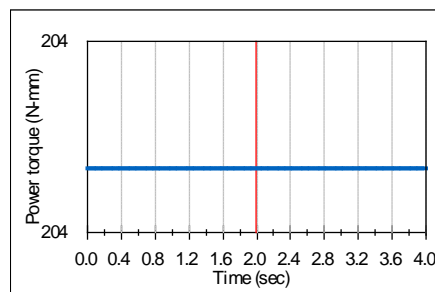


(a) Sliding ring (Output)

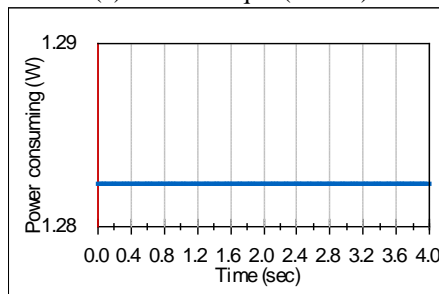


(b) Intermediary ring

Figure 2. Angle velocities of the components



(a) Power torque (N-mm)



(b) Power consumption (Watt)

Figure 3. Power needs for a loading of 100 Nm

3. FRACTURE ANALYSIS

The structural stresses of the reducer are studied for evaluating the fractures. Different failure modes

are likely to appear depending on the pitch-line velocity and transmitted torque. Possible failure modes of the gear ring occurring at positions of engagement of the gear teeth. The failure modes have both tooth breakage and tooth surface pitting as shown in **Figure 4**.

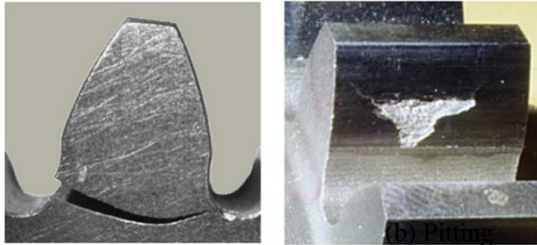


Figure 4. Fractured conditions of the gear teeth

3.1 Structural stress

The acted and reacted forces of the gear rings are illustrated as shown in **Figure 5**. Point P is the point of contact of the pitch circle of the intermediary and the sliding rings. The input torque (T_1) acting on the rotational center of the off-centre cam (O_1) drives the medium ring to rotate along with the fixed ring. The input torque will push the movement of the medium ring so that a reaction force (F_2) should arise at the point of contact of the pitch circle, P, due to the action of loading. As a result, the input torque (T_1) can then be decomposed into two components, the moment (T_2) and the horizontal force (F_2), acting on the center of the intermediary ring.

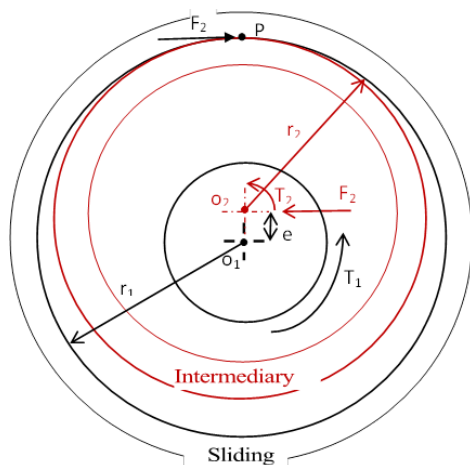


Figure 5. Loading analysis of the gear rings

The horizontal force can be obtained by taking the force equivalence as follows (Tsai et al., 2017):

$$F_2 = \frac{T_1}{(r_2 + e)} \quad (3)$$

The action of the moment on the intermediary ring can also be obtained by taking the moment equivalence as follows:

$$T_2 = \frac{r_2}{(r_2 + e)} T_1 \quad (4)$$

Breakage of the gear teeth is caused when the Root Bending Stress (**RBS**) exceeds the strength of the materials. Pitting of tooth surface is incurred by repeated surface contact stress (**SCS**). Increasing the transverse contact ratio as well as enlarging the overlap between the tooth contact-pairs is effective approaches to reducing noise and vibration. Generally, the **RBS** is commonly evaluated based on the Lewis equation. The gear tooth is modeled as taking the full load at its tip as with a simple cantilever beam. The **SCS** is commonly predicted based on Hertz theory in which the contact points are simulated as two contacting cylinders.

The analysis of gear stress usually necessitates the use of professional techniques and complex procedures. The ISO standard 6336-3 (1996) has already reported methods for the calculation of **RBS** and **SCS** for a pair of spur gears and helical gears. The formula of the **RBS** is obtained by extending the Lewis equation and considering some environmental factors by

$$\sigma_F = \frac{F_t}{bm} Y_F Y_S Y_C Y_H K_A K_D K_{F\alpha} K_{F\beta} \quad (5)$$

where

- F_t : the nominal tangential load (N),
- b : the face width (mm),
- m : the normal module (mm),
- Y_F : the form factor,
- Y_S : the stress correction factor,
- Y_C : the contact ratio factor,
- Y_H : the helix angle factor,
- K_A : the application factor,
- K_D : the dynamic factor,
- $K_{F\alpha}$: the transverse load factor of bending,
- $K_{F\beta}$: the face load factor of bending.

The formula of the **SCS** for a pair of spur gears and helical gears having contact ratios in the range $1 < c < 2$ is defined by

$$\sigma_H = Z_p Z_o Z_e Z_c Z_H \sqrt{\frac{F_t \cdot (u \pm 1)}{bd} K_A K_D K_{H\alpha} K_{H\beta}} \quad (6)$$

where the "+" symbol in the equation applies to the meshing of two external gears, and the "-" symbol is used for the meshing of an internal gear and an external. The other symbols are as follows:

- d : the reference diameter (mm),
- u : the gear ratio (Z_2/Z_1),
- Z_p : the single pair tooth contact factor,
- Z_o : the zone factor,
- Z_e : the elasticity factor,
- Z_c : the contact ratio factor,
- Z_H : the helix angle factor,

K_{Ha} : the transverse load factor of contacting,
 $K_{H\beta}$: the face load factor of contacting.

The two formulas include a number of unknown parameters which are usually determined through complex analytical procedures. For a detailed explanation in giving the proper values for these parameters, the readers can refer to the data reported in ISO 6336. For example, the design variables for the paired gear rings are $z_1, z_2, b, m=48, 50, 10, 1$, respectively. The moment acting on the gear ring is $T_2=96$ Nm when the input torque is $T_1=100$ Nm. The parameters used in the example are set to $\{F_t, b, m, Y_F, Y_S, Y_C, Y_H, K_A, K_D, K_{F\alpha}, K_{F\beta}\} = \{4000, 10, 1, 1.5, 1.2, 0.89, 1, 1, 1, 1, 1\}$, respectively. Substituting these values into Eq. (5), the evaluated value of **RBS** for the gear rings would be $\sigma_F=640.8$ MPa. On the other side, the parameters of the contact formula are set to $\{F_t, Z, d, b, u, Z_p, Z_o, Z_E, Z_C, Z_H, K_A, K_D, K_{Ha}, K_{H\beta}\} = \{4000, 48, 48, 10, 1.04, 1, 1.9, 186.9, 0.97, 1, 1, 1, 1, 1\}$, respectively. Substituting these values into Eq. (6), the value of **SCS** for the gear rings is $\sigma_c=1392.6$ MPa. The values of the parameters used in this example are to refer to the Ref. (Marciniec et al., 2009).

3.2 Fatigue Curves

The procedure and formulas for estimating gear life for a high number of cycles had been reported in AGMA Standard 2001-D04. The evaluated models of fatigue life for bending stress and contact stress are formulated in terms of a stress cycle factor, Y_N and Z_N as shown in **Figure 6**. The slopes of the (log-log) load-life plot in the AGMA specifications indicated that with a decrease in the scale of the stress there is an increase in the lifetime.

The stress cycle factors represent the relationship between the loading capacity of the gear and the stress cycles. The formulation for evaluation of the factors is based on the fact that the induced stresses do not exceed the allowable stress for the material. The relationships between the allowable stress and the stress cycle factors are defined by

$$\sigma_F = \frac{\sigma_{F\lim} \cdot Y_N}{K_F \cdot Y_\theta \cdot Y_z}, \quad (7a)$$

$$\sigma_H = \frac{\sigma_{H\lim} \cdot Z_N \cdot Z_W}{K_H \cdot Y_\theta \cdot Y_z}, \quad (7b)$$

where σ_F : bending stress taking into account the fatigue strength [MPa],

σ_H : contact stress taking into account the fatigue strength [MPa],

$\sigma_{F\lim}$: allowable bending stress at the root [MPa],

$\sigma_{H\lim}$: allowable contact stress [MPa],

K_F : safety factor for bending strength,

K_H : safety factor for pitting,

Y_N : stress cycle factor for bending strength,

Z_N : stress cycle factor for pitting resistance,

Y_θ : temperature factor,

Y_Z : reliability factor,

Z_W : hardness ratio factor for pitting resistance.

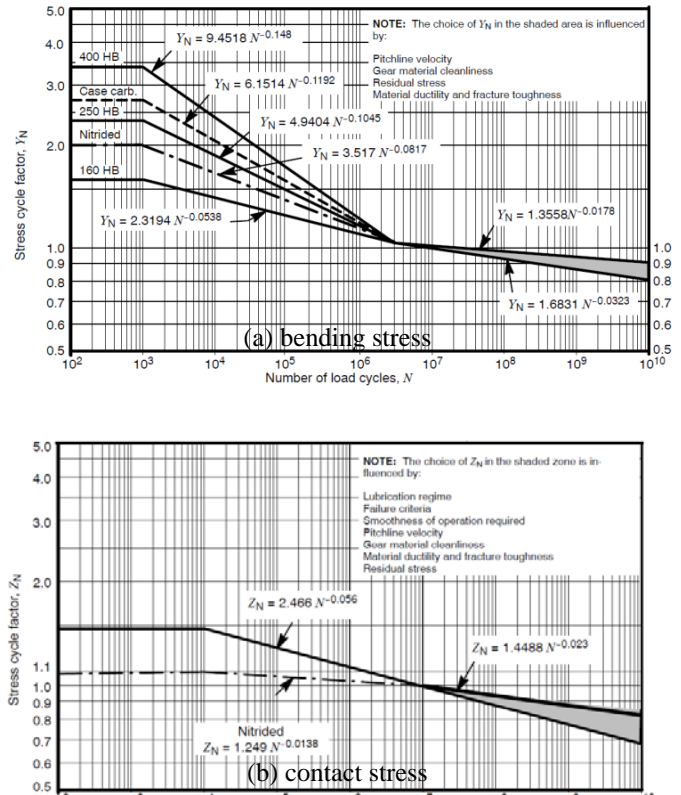


Figure 6. Fatigue life functions (AGMA,2004)

The stress cycle factors are dependent on the mechanical characteristics of the gear material such as the yielding strength, surface hardness and corrosion resistance, as well as the operational environment, such as the temperature, lubrication, etc. For details of the method for determining the values of the parameters related to the stress cycle factors, the interested reader can refer to the Ref. (AGMA,2004). For example, the allowable stresses for gears made of grade 1 hardened steel are rated by

$$\sigma_{F\lim} = 0.533H_B + 88.3, \quad (8.a)$$

$$\sigma_{H\lim} = 2.22H_B + 200.7, \quad (8.b)$$

where H_B is the Brinell hardness. The allowable stress has also been discussed in JGMA (1975).

4. FINITE ELEMENT METHODS

The geometric models obtained by SolidWorks are imported into ANSYS for models processing and performing stress analysis. The bending and contact stresses of the gear rings are the major concerned problems in the design. The maximum stresses obtained by FEM are compared with the evaluations by formula calculation to identify the accuracy of analyzing on stress.

The material of the gear rings is set to structural

steel. The geometric models including the inner-outer gear rings and the off-centre are loaded into ANSYS. The augmented Lagrangian formulation method is selected since it is the most suitable one for nonlinear analysis. The connection of the inner-outer gear rings are set to frictionless contact, and the cam to the inner ring is set to be bonded. A fixed support is placed at the outer gear ring as well as a frictionless support at the input hole of the off-centre cam. The gear thickness is set to 10 mm and the loading is set to be 100 Nm. The setting of the supports and the loadings are shown in Figure 7.

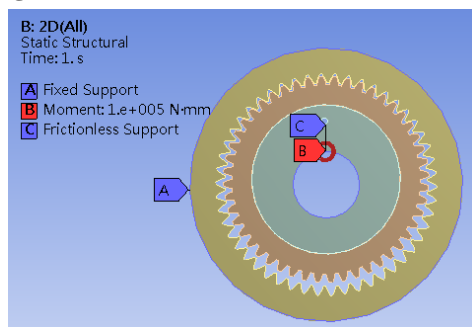


Figure 7. The analyzed settings

The interval of the mesh is set to 100 and the meshes in the areas of mating of the teeth are strengthened to obtain better solutions. The analyzed results for equivalent stress as well as the contact stress are shown in Figure 8.

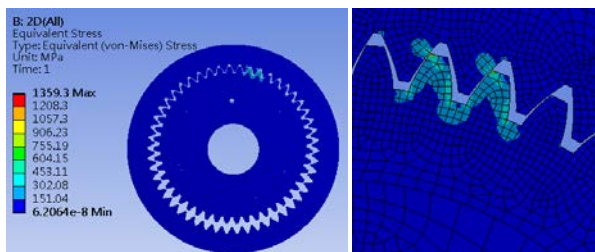


Figure 8. The surface contact stress

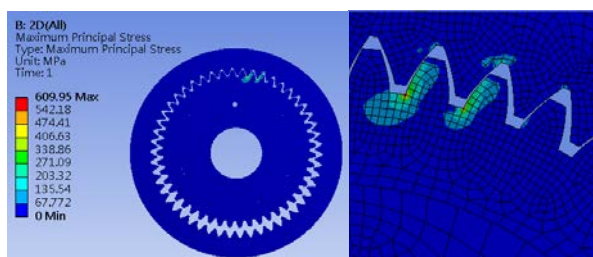


Figure 9. The root bending stress

The maximum value of the SCS for this example is 1359.3 MPa, occurring at the position of contact between the engaged teeth. The principle stresses as well as the bending stresses are shown in Figure 9. The maximum value of the RBS is 610 MPa, occurring at the tooth roots.

The contact stress may be varied during the engaging process due to the engaging point may have

different radius of curvature. In this paper, the contact locations of the tooth surfaces are simulated by setting the contact surfaces of the paired teeth as frictionless connections. On the other hand, the effects of the fillet shapes of the teeth generated by the rack cutter tip parameters are also ignored. The evaluated stresses would be smaller compared with the presented values if the fillets are considered. The evaluated results for maximum RBS and SCS are similar to the formula calculations reported in the previous section. The small errors between the evaluations imply that applying FEM to evaluate the RBS and SCS is practical.

Normally, the stresses in FEM analysis are closely related to the mesh settings. The convergence conditions of stress analysis based on the meshes of quadrilateral dominant are studied to identify the accuracy of analyzing. The maximum equivalent and principle stress for various element sizes are recorded in Table 1.

Table 1. The analysis results for various element sizes

Element Size (mm)	Mesh Nodes	Mesh Elements	Equivalent Stress	Principal Stress
2	15965	4870	558.1	400.8
1	16140	4923	628.1	484.7
0.8	16333	4990	631.2	478.1
0.5	16959	5188	926.7	513.5
0.3	18060	5541	1346.5	585.7
0.2	18673	5732	1358.1	609.8
0.1	19319	5950	1359.3	610.0

The convergence conditions about the maximum equivalent and principle stress are illustrated in Figure 10. The results show that the stresses will converge to one stable value. The results depict that making use of FEM to evaluate the structural stress of the reducer is acceptable.

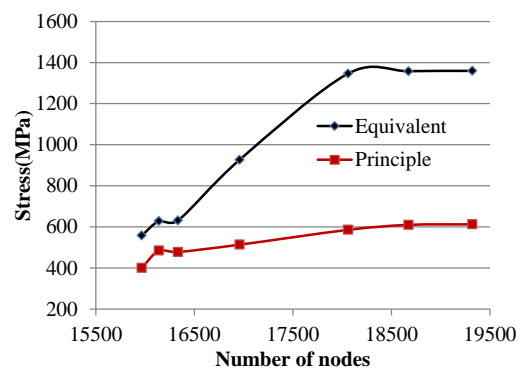


Figure 10. Convergence study

5. FATIGUE-LIFE PREDICTION

Fatigue life prediction usually is an approximate value because of the long testing times and the scatter of the experimental data. The

general methods for fatigue-life analysis are based on the data obtained from practical testing and statistical calculation (Tsai et al., 2015). In this study, a linear model which integrates the S-N curve with the fatigue curves reported in AGMA is proposed for evaluating the fatigue life of the gear rings.

(1). Bending fatigue

The linear form of fatigue-life estimation for bending stress is defined as follows:

$$\log(N_F) = -\frac{1}{b_F} [\log(a_F) - \log \sigma_F], \quad (9)$$

where a_F and b_F represent the strength coefficient and exponent of the materials, respectively. The b_F represents the slope of the line indicating the bending fatigue life trend (life line), which is determined according to the slopes of the life curves in AGMA models. They are derived from plotting the (log-log) stress cycle factor (Y_N) in comparison to the lifetime (N_F). The a_F is derived from the data for the second flexional point of the curves, i.e., $N_F=3*10^6$ cycles against the allowable bending stress (σ_{Flim}). The evaluations of the stress cycle factor, Y_N , and the coefficients of bending fatigue (a_F , b_F) for three materials H_B (160, 250, 400) are recorded in **Table 2**.

Table 2. Coefficients for bending fatigue

H_B	Y_N (10^3)	Y_N ($3*10^6$)	σ_{Flim}	a_F	b_F
160	1.6	1.04	177	394	-0.053805
250	2.4	1.04	227	1076	-0.104448
400	3.4	1.04	310	2812	-0.147952

The trend lines of parameter changing in terms of material hardness H_B are derived by linear regression methods. The trend lines are illustrated in **Figure 11**. The equations for calculation of the life parameters are defined as

$$a_F = 0.0167x^2 + 0.731x - 149.58, \quad (10.a)$$

$$b_F = -0.1027\ln(x) + 0.4656, \quad (10.b)$$

where x is the hardness of material (H_B). The above equations are used to evaluate the bending fatigue life of the gear ring after the life coefficients determined according to the material hardnesses.

(2) Contact Fatigue

The specifications of the relationship between the contact life factors and the fatigue life reported in AGMA standards are used. The slope of the (log-log) load-life plot indicates that an increase in the load of 2% leads to a fatigue life reduction of 30%. The values of the flexional points are $Z_N(1.47)$ against $N_H(10^4)$ as well as $Z_N(1)$ against $N_H(10^7)$. According to the definition, the model for contact fatigue

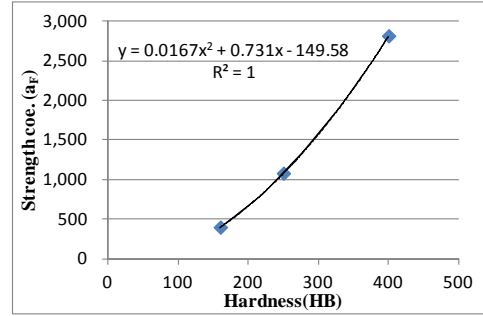
lifetime can be defined as

$$\log(N_H) = 17.93[\log(a_H) - \log(\sigma_H)]. \quad (11)$$

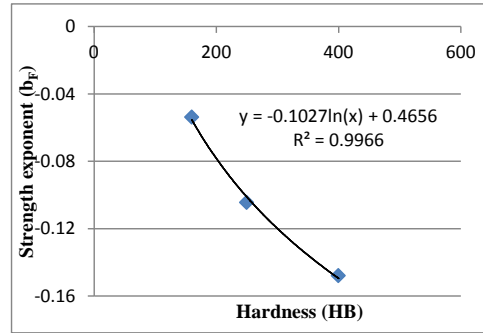
The parameter, a_H , can be rated according to the values of the second flexional point as

$$a_H = 2.457\sigma_{Hlim}. \quad (12)$$

where σ_{Hlim} is the allowable contact stress. As soon as the parameters are decided, the contact fatigue lifetimes can be evaluated.



(a) a_F



(b) b_F

Figure 11. Trending lines of bending fatigue

The estimations of fatigue life by the linear models and by the AGMA curves are compared. Three materials H_B (160, 250, 400) are considered for comparison. The evaluations include the allowable stress (σ_{Flim} , σ_{Hlim}), the fatigue lifetime and the errors for the two models at someone stress (σ_F , σ_H) are listed in **Table 3**.

Here, the parameters indicating the stress cycle factors (K_F , K_H , Y_θ , Y_Z , Z_W) for evaluation of the curves in AGMA are all set to be equal to 1. The evaluated results show that the predicted log errors of the lifetimes between the linear model and the curves in AGMA are small. The predicted lifetimes related to contact stress for the two models are almost the same. The maximum evaluated errors at the boundary point are about 3 percent of the log AGMA lifetimes. The results imply that the linear model can be used to predict the fatigue lifetimes of the gear rings used in the reducer. The linear model is more convenient than the AGAM model because it can directly predict the fatigue lifetimes from the material hardness (H_B).

Table. 3 The lifetime as estimated by the linear model and the AGMA model

Stress types	H_B	σ_{Flim}	σ_F	AGMA model		Linear model			Predicted Errors (log)
		σ_{Hlim}	σ_H	$Y_N (Z_N)$	Lifetime	$a_F(a_H)$	$b_F(b_H)$	Lifetime	
Bending	160	177	177	1.0413	2,915,577	394.9	-0.0556	1,844,767	-3.07%
Contact		556	656	1.1799	521,197	1365.8	-0.0558	515,058	-0.09%
Bending	250	227	227	1.0421	2,935,125	1076.9	-0.1015	4,620,289	3.05%
Contact		756	856	1.1323	1,086,647	1856.8	-0.0558	1,077,071	-0.06%
Bending	400	310	310	1.0417	2,961,334	2814.8	-0.1497	2,506,450	-1.12%
Contact		1089	1089	1.0003	9,948,087	2674.9	-0.0558	9,949,907	0.00%

6. RELIABILITY EVALUATION

The material properties of the reducer including the strength, hardness and the allowable stresses must be given before evaluating the fatigue lifetime. In this case, the materials of the gear rings are designed of structural steel, S45C, where the tensile and yield strength and the hardness are $\sigma_{ut}=627$ MPa, $\sigma_{yp}=355$ MPa and $H_B=200$, respectively. The allowable bending and contact stress, as evaluated by Eq. (8), are $\sigma_{Flim}=199$, $\sigma_{Hlim}=645$ MPa, respectively. The suggested values for normalized structural steel without case hardening (S45C, $H_B=200$) are $\sigma_{Flim}=196$, $\sigma_{Hlim}=505$ MPa obtained from JGMA. Comparing both models, we find that the allowable bending stress is almost the same but the allowable contact stress suggested by JGMA is more conservative than in the AGMA specifications. In this study, the allowable stress of the AGMA specifications is used in the evaluation of the fatigue lifetime of the reducer.

The maximum **RBS** and **SCS** for loadings from 20-100 Nm evaluated by ANSYS are shown in Table 4. The allowable stress and the life coefficients for the material $H_B(200)$ are shown in the lowest row. The fatigue lifetimes are obtained by substituting the evaluated stress into the linear models.

Table 4. The stresses and lifetimes at different loads

T1 (Nm)	Bending (MPa)	Contact (MPa)	Total defor.	Bending lifetime	Contact lifetime
20	130	314	0.005	1.07E+9	4.09E+12
30	195	472	0.008	6.14E+6	2.71E+9
40	260	628	0.010	1.54E+5	1.60E+7
50	328	772	0.013	8.03E+3	3.97E+5
60	396	916	0.015	7.32E+2	1.84E+4
70	464	1061	0.018	9.76E+1	1.32E+3
80	517	1169	0.020	2.47E+1	2.33E+2
90	563	1264	0.022	8.21E+0	5.75E+1
100	610	1359	0.023	2.98E+0	1.55E+1
H_B	$\sigma_{F,lim}$	$\sigma_{H,lim}$	$a_F(a_H)$	664.6	1584.0
200	199	645	$b_F(b_H)$	-0.078537	-0.055772

The results show that bending fractures are more likely to occur in the gear rings prior to contact

fractures. For example, an input torque $T_1=40$ Nm, the bending stress will exceed the allowable value σ_{Flim} , however, the contact stress is still within the allowable value σ_{Hlim} . The allowable loading for the reducer is about at 30 Nm and the yield loading is about 55 Nm, where the maximum **RBS** matches the yield strength σ_{yp} . The results show that the bending lifetime is also shorter than the contact lifetime. The effects of the thickness of the material are also shown. The estimated lifetimes of the reducer with different material thicknesses under a loading of 50 Nm are shown in Figure 12.

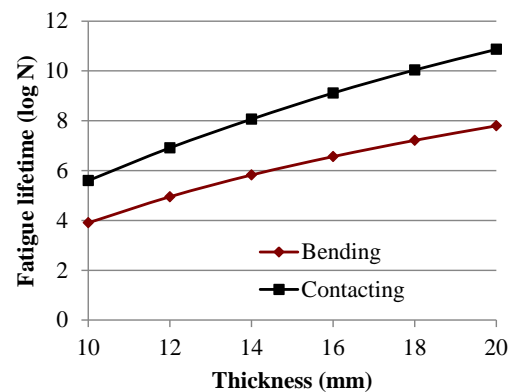


Figure 12. Fatigue lifetimes for various thicknesses

The results indicate that failures of the reducer are primarily related to the **RBS** and the bending fatigue lifetimes are shorter than the contact fatigue lifetimes.

The reliability of the reducer in use can be further determined by considering the distribution of the lifetimes. The distribution of estimated fatigue lifetimes given the variation of material strength is determined. The characteristic parameters of the life distributions can be derived for variations in material hardness. Here, bending fatigue lifetime is considered when evaluating the reliability, since it is shorter than the contact fatigue lifetime.

Fatigue lifetimes are usually expressed as lognormal distributions. Combining the estimated values of $P=50\%$ lifetime and the standard deviation of the estimations, the reliability of the fatigue life corresponding to different loads can be computed. The parameters for determining the lifetime lognormal

distributions are (μ_Y, σ_Y) . The parameters can be estimated by

$$\begin{aligned} \mu_Y &= \log \mu_X - \frac{1}{2} \sigma_Y^2 \\ \sigma_Y^2 &= \log \left[\left(\frac{\sigma_X}{\mu_X} \right)^2 + 1 \right], \end{aligned} \tag{14}$$

where μ_X and σ_X are the mean and the standard deviation of the lifetimes with a normal distribution. The standard deviation of the fatigue life σ_Y can be obtained from the above equations as well as the mean representing the 50% lifetime, as $\mu_Y = \log(N)$.

In this example, the mean and the standard deviation of the hardness of the material, S45C, are about $\mu_B, \sigma_B=200, 20$, respectively, according to the data in JGMA. The variation of the coefficients of the linear model can be obtained by the distribution join operations (Tsai et al., 2008). In particular, the evaluation results of the means and standard deviations of the life coefficients and the log lifetimes of the gear ring for **RBS**, 200 MPa, are listed in **Table 5**

Table 5. The evaluations of life coefficients for bending stress (200 Mpa)

Dist.	a_F	b_F	$\log(N)$
μ	664.62	-0.0785	6.6407
σ	148.22	0.0103	1.4684

Given the characteristic parameters for the life distribution, the fatigue reliability of the reducer can be evaluated by Tsai et al.(2013)

$$R(t) = \Phi \left(\frac{\log(N) - \mu_Y}{\sigma_Y} \right). \tag{15}$$

The estimated means and the variations of the fatigue lifetimes for several **RBS** are listed in **Table 6**. The degradation in the reliability of the reducer when subjected to three levels of stress can be computed by the above equation, with the results shown in **Fig. 15**. The study results show the standard deviation of the material’s cyclic properties which have a great effect on the reliability degradation. The proposed approach can be used to determine the risk and the maximum permissible loading for the reducer.

Table 6. The fatigue lifetimes at various stresses

Stress	200	250	300
N	4,372,388	255,141	25,037
logN	6.6407	5.4068	4.3986
$\sigma^2_{\log N}$	2.1563	1.9021	1.7331

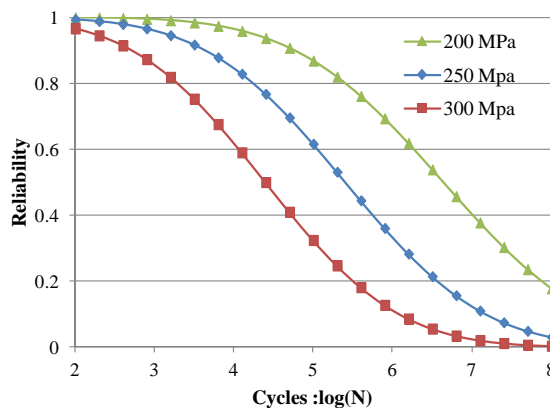


Figure 15. Reliabilities of fatigue lifetime at various loads

7. CONCLUSIONS

This paper reports the design and fatigue-life prediction for a high-ratio speed reducer. The geometric structure of the reducer, including simulation of the motion, is examined through the modeling processes. The structural stresses including the **RBS** and the **SCS** of the gear rings are studied to obtain the allowable loadings of the design. **FEM** is used as a tool to analyze the induced stresses of the reducer for different material thicknesses and loadings. A linear model for fatigue-life prediction is proposed using the S-N curve with the life information reported in the AGMA Standards. The linear model provides a simple method for fatigue-life prediction according to the stresses obtained in **FEM** analysis and material hardness. The studied results show that failures of the reducer are primarily related to the **RBS** of the gear rings, and the bending lifetime is also shorter than the contact lifetime. The evaluated methods of the mean and the standard deviation of the lifetimes are derived based on material strength distributions. Reliability degradation of the reducer at various loads are further studied. The results of the study provide useful information for designing, structural stress analysis, fatigue-life prediction and reliability evaluation for developing a high performance reducer.

ACKNOWLEDGEMENTS

This work was supported by a grant from the National Science Council under contract No: MOST 104-2221-E-237-001. The authors would like to express their appreciation to the reviewers for their valuable suggestions which have helped to greatly improve the manuscript.

REFERENCES

Alban L. E., “Systematic analysis of gear failures”, *American Society for Metals* (1993).

- ANSI/AGMA Standard 2001-D04, "Fundamental rating factors and calculation methods for involute spur and helical gear teeth" (2004).
- ANSYS user's manual, ANSYS Inc. (2012).
- Ciavarella M. and G. Demelio, "Numerical methods for the optimisation of specific sliding, stress concentration and fatigue life of gears", *International Journal of Fatigue*, Vol.21, pp.465-474 (1999).
- Ghorbel, F. H., P. S. Gandhi and F. Alpeter, "On the kinematics error in harmonic drive gears", *Journal of Mechanical Design*, Vol. 123, No.1, pp.90-97 (2001).
- ISO Standard 6336-1, 2, 3: Calculation of load capacity of cylindrical gears (1996).
- JGMA 402-01, "Surface durability formula of spur gears and helical gears", *Japanese Gear Manufacturer Association (JGMA)*, (1975).
- Kader, M. A., S. P. Nigam and G. K. Grover, "A study on mode of failure in spur gears under optimized conditions", *Mech. Mach. Theory*, Vol. 33, pp.839-850 (1998).
- Lee, Y. L. and J. Pan, "Fatigue testing and analysis - Theory and Practice", *Elsevier Butterworth-Heinemann*, New York, (2005).
- Marciniec, A. and A. Pawlowicz, "The bending and contact stress analysis of spur gears", *Journal of KONES Powertrain and Transport*, Vol.16, No.3, pp.243-250 (2009).
- Robert, D. C., "Concepts and applications of finite element analysis", *John Wiley and Sons, Inc.*, New York, (2001).
- Shuting Li, "Design and strength analysis methods of the trochoidal gear reducers", *Mechanism and Machine Theory*, Vol. 81, pp.140-154 (2014).
- Taghirad, H. D. and P. R. Belanger, "Modeling and parameter identification of harmonic drive systems", *Journal of Dynamic Systems, Measurement and Control*, Vol.120, No.4, pp. 439-444 (2009).
- Thompson, D. F., S. Gupta and A. Shukla, "Trade-off analysis in minimum volume design of multi-stage spur gear reduction units". *Mech. Mach. Theory*, Vol.35, pp.609-627, 2000.
- Tsai, Y.T. and Y.M. Chang, "Function-based cost estimation of systems integrating quality function deployment", *International Journal of Advanced manufacturing technology*, Vol.23, No.7-8, pp.514-522 (2004).
- Tsai, Y.T. and H.C. Chang, "Reliability-based optimum design for mechanical problems using genetic algorithms", *Proc. IMechE, Part C: J. Mechanical Engineering Science*, Vol.222 (C9), pp.1791-1799 (2008).
- Tsai, Y.T., K.S. Wang and J.C. Woo, "Fatigue-life and reliability evaluations of dental implants based on computer simulation and limited test data", *Proc. IMechE, Part C: J. Mechanical Engineering Science*, Vol.227, No.3, pp. 554-564 (2013).
- Tsai, Y.T., K. H. Lin and Y.Y. Hsu, "Reliability optimization design for mechanical devices based on modeling processes", *Journal of Engineering Design*, Vol.24, No.12, pp.849-863 (2013).
- Tsai, Y.T. and K.S. Wang, "A study of reliability analysis of fatigue life for dental implants", *Journal of Chinese Society of Mechanical Engineers*, Vol.36. No.5, pp.439- 448 (2015).
- Tsai, Y.T. and K. H. Lin, "Structural stress analysis and reliability evaluation for a new speed reducer", *Journal of Mechanics*, Vol.33, No.5, pp.631-640 (2017).

減速裝置設計和疲勞壽命 預估

蔡有藤

宏國德霖科技大學機械系

林寬泓

東南科技大學機械系

王國雄

國立中央大學機械系

摘要

這研究發表高減速比減速裝置結構應力分析和疲勞壽命預估方法，它包含：(1)減速器的設計和運動模擬，(2)減速器齒根彎曲應力(RBS)及表面接觸應力(SCS)分析方法(ISO standard 6336-3)，(3)利用ANSI/AGMA模型和一個線性模型預估減速器彎曲和接觸疲勞壽命，(4)利用有限元素分析法(FEM)分析結構應力，用以預估減速器之疲勞壽命和可靠性退化。FEM分析應力和公式計算應力比較，驗證機構幾何模型設計正確性，利用ANSI/AGMA和一個線性模型預估減速裝置壽命，比較預估壽命差異；應力分析結果顯示，減速器的疲勞失效主要由彎曲應力造成，依據FEM應力分析結果預估可靠度退化和疲勞壽命，決定裝置操作最大容許負載、不同負載下操作風險。本研究在機構設計、結構應力分析、疲勞壽命預估提供良好技術支援，對開發高減速比裝置提供相當助益。